Regional Studies in Marine Science 73 (2024) 103457

Contents lists available at ScienceDirect

Regional Studies in Marine Science

journal homepage: www.elsevier.com/locate/rsma

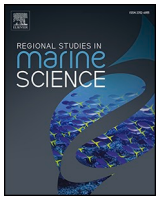

Influence of the Rhone River intrusion on microplastic distribution in the Bay of Marseille

A. Alcaïno [a,*], L. Vidal [a], L. Licari [a], C. Paillès [a], S. Conrod [a], J. Dauvier [a], C. Chevalier [b], C. Pinazo [b], M. Grelaud [c], P. Ziveri [c,d]

[a] Aix Marseille Univ, CNRS, IRD, CdF, INRAE, CEREGE, Aix en Provence, France
[b] Aix Marseille Université, Université de Toulon, CNRS, IRD, MIO, Marseille, France
[c] Institut de Ciència i Tecnologia Ambientals (ICTA-UAB), Universitat Autònoma de Barcelona, Cerdanyola del Vallès, Barcelona 08193, Spain
[d] Catalan Institution for Research and Advanced Studies (ICREA), Barcelona, Spain

ARTICLE INFO

Keywords:
Microplastics
Extraction protocol
Rhone River intrusion
Modelling
Mediterranean Sea

ABSTRACT

We present the spatiotemporal distribution of microplastics (MP) in surface waters and sediments between 2020 and 2022 in the Bay of Marseille. Microplastics were extracted with an improved, ecological protocol from 27 surface water and 16 sediment samples. The hydrodynamical circulation model MARS3D-RHOMA was used with *in-situ* data to test the influence of meteorological and hydrodynamic forcing on the concentration of MPs during the study period. The reported concentrations are analogous to abundances previously found in the Bay of Marseille, as well as in similar coastal systems. Average MP concentrations are 5.79 ± 12.71 MP.m^{-3} in surface water and 855 ± 413 MP.kg^{-1} dw in sediments. Simulations revealed hydrodynamic features associated with several episodes of Rhone intrusion in the Bay of Marseille. The observed MP concentrations and distribution in February 2020 suggest that the Rhone River's plume entered the Bay of Marseille.

1. Introduction

The world plastic production has increased from year to year, reaching 390.7 million tons in 2021 (Plastics - the Facts, 2022, s.d.) and 4.8–12.7 million tons are assumed to enter the ocean annually (Jambeck et al., 2015). Plastics have contaminated all compartments of the marine environment from the highly populated coastlines to the sea floor bottom where they accumulate (Galgani et al., 1995; Hess et al., 1999; Galgani et al., 2000; Kane and Clare, 2019; Simon-Sánchez et al., 2022b). The implications of plastic pollution are multiple, from the strangulation of marine species (Laist, 1987) to the transport of persistent organic pollutants (POPs) (Mato et al., 2001) and exogenous species (Barnes, 2002).

Microplastics (MP) or plastic items <5 mm, represent about 92% of marine plastic (Eriksen et al., 2014). They are manufactured (primary MPs) or derived from the fragmentation of macroplastics (secondary MPs). They enter the marine environment through various pathways (water runoff, river discharges, or atmospheric deposits) and accumulate in marine waters and sediments (Thompson, 2004), contaminating all the ocean reservoirs (Coyle et al., 2020). MPs are a complex mixture of polymers and additives, capable of easily transporting contaminants because of their specific physical properties (Teuten et al., 2009). The exposure of marine organisms to MPs alters their fertility, their feeding behaviour, or CO_2 absorption (Galloway et al., 2017; Seuront et al., 2022).

Studies on plastic and MP pollution have grown exponentially since the early 2000 s. However, the protocols used are as diverse and numerous as the studies themselves, and no standard protocol exists to extract, quantify, and characterise MPs (Cutroneo et al., 2020; Seuront et al., 2022; Simon-Sánchez et al., 2022a). As a result, the sampling methods and extraction protocols can lead to an underestimation of certain MP types such as fibres (Barrows et al., 2017; Ryan et al., 2020) thus compromising inter-site comparisons.

The Mediterranean Sea hosts 150 million inhabitants, undergoes mass tourism, industrialisation, intense shipping, and fishing activities (Fabres et al., 2012), and is thus under high anthropogenic pressure. It is particularly affected by plastic contamination, making it the most plastic and MP polluted sea in the world (Cózar et al., 2015; Cincinelli et al., 2019). This situation is mainly due to its geomorphology as a semi-enclosed basin with an anti-estuarine circulation and reduced

* Corresponding author.
E-mail address: alcaino@cerege.fr (A. Alcaïno).

https://doi.org/10.1016/j.rsma.2024.103457
Received 30 September 2023; Received in revised form 26 February 2024; Accepted 27 February 2024
Available online 2 March 2024
2352-4855/© 2024 Published by Elsevier B.V.

communication with the Atlantic Ocean through the Strait of Gibraltar. Moreover, it receives continental water discharges from highly urbanised countries, some with poor waste (water) management, contributing further to its plastic pollution (Lebreton et al., 2017; Cincinelli et al., 2019).

To manage and mitigate this issue, it is critical to precisely quantify and characterise the amount of MPs in the Mediterranean Sea and their possible sources. Despite an increasing number of studies on MP pollution in the Mediterranean Sea, only a few have focused on Marseille given the complexity of the site (Collignon et al., 2012; Gérigny et al., 2022; Henry and Galgani, 2013; Schmidt et al., 2018, 2021; Tsiaras et al., 2022). Most surveys analyse MP contamination based on punctual surficial water samples while analyses of MP contamination in sediments are scarce (Ourgaud et al., 2022). Another challenge is to understand the processes controlling MP distribution in areas where forcing factors are diverse and variable, acting at different time scales (diurnal, seasonal and interannual). In the Bay of Marseille, while the diurnal variability (tides) is negligible, hydrodynamical complexity results from various forcing factors (e.g. variable wind patterns, northern current and Rhone River plume intrusions; Allou et al., 2010; Gatti et al., 2006; Petrenko et al., 2008). In this context, hydrodynamic and Lagrangian transportation models have proven to be powerful tools to understand the distribution and transport of MP particles (Tsiaras et al., 2022; Zayen et al., 2020).

In this paper, we present for the first time, based on a 3-year survey (2020–2022), a comprehensive dataset on MP quantification and characterisation in the Bay of Marseille from water and sediment samples. To tackle the hydrodynamic forcing on MP distribution, we used a high-resolution model simulation MARS3D-RHOMA (Fraysse et al., 2013) updated for the monitored period. Comparisons with different hydro-meteorological forcings were tested as well as particle trajectory simulations with Ichthyop software (Lett et al., 2008). Monitoring and model simulation provided new insights into the episodic influence of the Rhone River plume on MP distribution in the Bay of Marseille. Our results are compared to previous work in the Bay of Marseille and to international studies with comparable geographic environments.

2. Material and methods

2.1. Study area characteristics

The Bay of Marseille is in the eastern part of the Gulf of Lion (western Mediterranean Sea, France). The Bay is naturally delimited by two calcareous units: the Calanques mountain range (National Park) on the eastern side and the Nerthe mountain range (Côte Bleue) on the western side. Offshore, Planier island limits the Bay (Fig. 1). The Bay is divided in two parts by the Frioul islands: the northern Bay and the southern Bay that are distinct in terms of occupation. The northern part is mainly dedicated to cruise terminals, ship repair basins and warehouses whereas the southern part hosts beach facilities and marinas. The two areas are characterised by contrasted rates of land artificialization: 92% and 23% of their surface respectively for the northern and southern bay (AGAM, 2016).

Marseille is the largest port in France. The city covers a large area (240.6 km^2) and is densely populated (3 587.9 inhabitants/km^2, INSEE 2017), with intense shipping, cruising, and fishing activities. In addition to urbanisation, two urban creeks, the Aygalades and the Huveaune, discharge respectively in the commercial part of the Bay and in the Calanques National Park. The Huveaune drains a 520 km^2 basin, populated with more than 1 million inhabitants (25% urbanised and 2% industrialised - Epage HuCA), and has been connected since 1976 with Marseille's main WWTP outlet located in the Calanques National Park (Cortiou). Most of the time, with an average waterflow of 2 $m^3.s^{-1}$, the creek discharges into the Cortiou calanque. During heavy rain episodes, the waterflow increases (>30 $m^3.s^{-1}$), and the Huveaune creek discharges sporadically near the Prado beach (Tramoy et al., 2022). Although not monitored, the Aygalades creek has a low waterflow. It drains a 50 km^2 catchment (55% urbanised) and discharges into the commercial port of Marseille. However, the Aygalades creek is polluted from its source because of quarrying and chemical industries in the Maire valley.

Hydro-meteorological conditions in the Bay of Marseille are highly variable with extreme events that are typical of a Mediterranean climate. Average annual rainfall is 545 mm. However, flash storms can bring 80–100 mm in a few hours. The Bay is subject to diverse wind regimes, but the strongest winds are the Mistral (cold and dry N-NW wind) and a S-SE wind (warm and humid) (Millot, 1990). Wind direction shifts are frequent. The hydrodynamics in the Bay of Marseille is strongly influenced by the N-NW winds and the S-SE winds that favour, respectively, up and downwelling near the Calanques and the Côte Bleue (Millot, 1990; Odic et al., 2022). During specific hydrodynamic events, episodic eutrophic freshwater intrusions from the Rhone River plume were observed to enter the Bay and transfer organic matter and microparticles (Gatti et al., 2006; Millet et al., 2018; Schmidt et al., 2020). In this area, the tidal currents are of small amplitude and negligible (Millot, 1990).

The mouth of the Rhone River, located 35 km away from the Bay of Marseille, is one of the largest inputs of freshwater and nutrients into the Gulf of Lion, with a mean outflow of 1710 $m^3.s^{-1}$. Although it does not flow directly into the Bay, the Rhone River impacts the hydrodynamics of the Bay by its plume extension. Due to the Coriolis effect, the Rhone plume extends normally to the west, but under a N-NW wind regime it

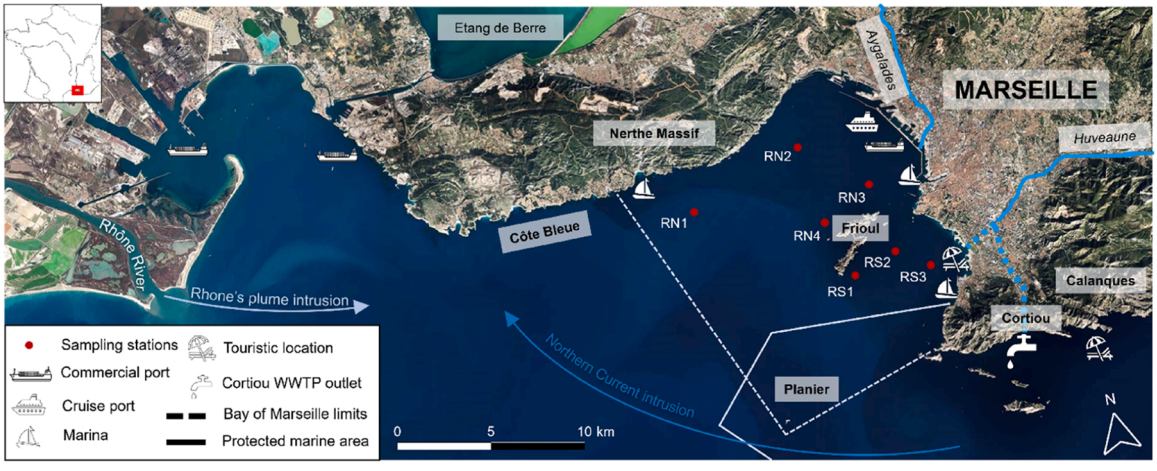

Fig. 1. Sampling stations in the bay of Marseille and main forcing (satellite picture: Science Photo Library).

extends to the south whereas under a S-SE wind regime it extends to the east, along the northern coastline into the Bay of Marseille (Demarcq and Wald, 1984).

Extensive simulations performed with the MARS3D-RHOMA model showed that these intrusions appeared to be driven by a combination of several favourable factors: wind forcing, the presence of a sub-mesoscale eddy, a sufficient Rhone River discharge, variations in thermocline depth and when the salinity is under the 37.8 threshold (Fraysse et al., 2014). Rhone intrusions are therefore common with about 7 intrusions per year, lasting 3 days in average, and occurring mainly in summer and at the beginning of autumn. In addition, under a SE wind regime, the Northern current flow can bring microparticles from the east and particularly from the Cortiou WWTP (Millet et al., 2018).

2.2. Sampling methodology

Seven sites were sampled seasonally (spring and autumn) during a 3-year survey (02/ 2020, 09/2020, 03/2021, 09/2021, and 03/2022) on board CNRS-INSU R/V Antédon II. In the northern Bay four sites were selected: two sites in the path of the Rhone River plume (RN1, RN2), one in the vicinity of the commercial port (RN3) and one close to the Frioul islands (RN4). In the southern bay, three sites were selected near the most touristic places and marinas (RS1, RS2, RS3) with intense marine activities and in the path of the intrusion of the Northern Current.

Water and surface sediment were sampled at each site. Sample location was geolocalised with the GPS system of the R/V Antédon II. The surface water was collected by towing a manta trawl with an opening of 0.15×0.50 m with 330 μm mesh size at an average speed of 2 knots during a 20-minute circular path. The average water volume collected for each manta sample was 86 m^3 (Supplementary data). The manta net was then rinsed with filtered seawater to gather sampled material which was transferred into a glass jar using filtered distilled water (0.22 μm). Surface sediment was collected using a Van Veen grab sampler. The uppermost layer of unconsolidated sediment was transferred with a metal spoon into a glass jar. Samples were stored at 4°C until analysis.

2.3. Extraction

The MP extraction protocol was done following Masura et al. (2015), although some modifications were added to quickly extract MP from sea water and sediment samples from our study site. All experiments were carried out with filtered distilled water (0.22 μm).

2.3.1. Adapted Protocol and validation

The main steps from the Masura et al. (2015) protocol are: sample wet sieving between 250 μm - 4 mm, oven dried at 50°C during 24 h, oxidation (WPO) of 120 mg of the dry sample with 20 ml of $FeSO_4$ and as much H_2O_2 as necessary (50 ml by 50 ml), NaCl densimetric separation of the sample, filtration of the light fraction on a 0.45 μm gridded filter for the analysis. Two steps were adapted here to reduce the duration and the amount of chemicals used.

An intermediate sieving at 250 μm was introduced during the WPO to remove fine organic compounds. This reduced the volume of H_2O_2 used by 17%. As this step did not change the MP counts significantly after extraction (Fig. S1), we shifted to a smaller sieve mesh (63 μm). In this case, the H_2O_2 volume was reduced by 75%. No significant differences were observed in the MP counts (Fig. S1) and visual inspection of the <63 μm fraction confirmed that there were no MPs in the size range 250 μm – 4 mm, nor any fibres that passed through the sieve due to their small diameter. While the density separation was maintained for the extraction of the MP from the sediment samples, this step was considered too time-consuming and not efficient enough for water samples in view of the low organic matter content in the surface water. For water samples, direct sieving after the digestion at 63 μm was preferred to an overnight NaCl density separation, without any impact on the MP counts (Fig. S1). Lastly, this protocol, adapted so as to be suitable for the environmental context of the Bay of Marseille, reduced the use of chemicals, and is more eco-friendly and fitting for potential use in participatory sciences.

2.3.2. Contamination control

Contamination needs to be carefully considered during sample collection and preparation. MP can be cloth-derived, airborne, or attached to operating equipment. Therefore, operators wore a fuschia-pink cotton lab coat to enable natural fibre contamination to be easily spotted. During on board sampling, an open Petri dish with a gridded filter was placed nearby and covered once sampling had resumed. Sampling and laboratory equipment were thoroughly pre-washed with 0.22 μm filtered distilled water and as far as possible plastic-free dishware, except for the Teflon wash bottle and the stockage tubes, was used. Samples were kept covered with watch glass whenever possible. Controls/blanks using filtered distilled water and washed (450°C) diatomaceous earth were run in parallel as analytical blanks. In addition, during the laboratory manipulations, whenever the sample was uncovered or was being transferred, a Petri dish with a gridded filter was left open to assess ambient microplastics in the air.

2.3.3. Water samples

Once in the laboratory, the > 330 μm size fraction was successively sieved at 4 mm and 250 μm and rinsed to remove sea salt, macro debris and fine material. The > 4 mm size fraction was dried and stored in a glass vial. The > 250 μm size fraction was resuspended in 100 ml of filtered distilled water and transferred into a Folsom sampler to be split into two 50 ml sub-samples. The 50 ml aliquots were either frozen until further analysis or immediately transferred into a beaker for WPO.

To remove organic matter, 20 ml of aqueous 0.05 M Fe (II) solution and 50 ml of 30% H_2O_2 were added to the >250 μm size fraction. After a boiling reaction, the mixture was sonicated to further break down the organic compounds. Once cooled, another 50 ml of hydrogen peroxide were added with sonication after the boiling reaction. The mixture was then sieved at 63 μm to collect the non-digested particles. The >63 μm size fraction was resuspended in filtered distilled water, and vacuum filtered on a 0.45 μm gridded cellulose filter. The filter was placed in a Petri dish and dried overnight at room temperature.

2.3.4. Sediments

For each sediment sample, a small quantity was dried overnight at 50°C in a pre-weighed aluminium weighing tray. After drying and weighing, the amount of wet sediment corresponding to 100 g of dry sediment was placed in a sealed glass container with 20 ml of clay dispersing agent and filtered distilled water and left to rotate for 2 h. The sediment mixture was then successively sieved at 4 mm and 250 μm and rinsed to remove sea salt, macro debris and fine material. The > 4 mm size fraction was dried and stored in a glass vial. The > 250 μm size fraction was resuspended in 200 ml of 5 M NaCl solution. After decanting for one hour, the supernatant was collected with a glass pipette and transferred into another clean beaker. This step was repeated twice. The supernatant was then vacuum filtered on a 180 μm filter to eliminate the NaCl solution. The >180 μm size fraction underwent wet peroxide oxidation and the final step of 0.45 μm filtration, like the sea water samples.

2.4. MP identification and chemical characterisation

After extraction, MPs collected on gridded filters were observed under a binocular microscope (LEICA). To rule out non-plastic fragments, each particle was submitted to a pressure test with inox forceps and a fusion test with a heated needle. Each MP was classified following Masura et al. (2015). The type (fibre, fragment, film, and foam), colour and size class were recorded. The size was determined using the 3 mm-squares on gridded filters. MPs were classified following 13 size

classes: from 0.5 mm to 5 mm with an interval of 0.5 mm between each class, with additional size classes of <0.25 mm, 0.25 mm and >5 mm. On each filter, all suspected MPs were counted, collected, and stored in a glass vial. For surface water, MPs were expressed in units of MP per cubic metre (MP.m^{-3} - and MP.km^{-2}) and for sediment samples in MP per kilogram of dried weight sediments (MP.kg^{-1} dw). The chemical characterisation of surface and sediment samples was performed with an Agilent Cary 630 ATR-FTIR (ICTA-UAB, Barcelona, Spain). For technical constraints, we selected dominant MPs larger than 250 μm. In the case of fibres, similar items were gathered. A total of 155 particles were analysed collected during three sampling campaigns (February 2020, March 2021, September 2021). For the surface water samples 105 particles were analysed (43 fibres, 33 fragments, 17 foams, 12 films). For the sediment samples 50 particles were analysed (33 fibres, 5 films, 7 fragments, and 5 foams).

2.5. Hydrodynamic model and surface dispersal modelling

To simulate the hydrodynamic conditions in the Bay of Marseille before and during our sampling period, the MARS3D-RHOMA model configuration (Pairaud et al., 2011; Fraysse et al., 2013) and the model visualizer SimuXplorer (created by Vincent Faure, MIO; Garnier et al., submitted) were used. The hydrodynamic model used for this study was the free surface, three-dimensional MARS3D model (3D hydrodynamic Model for Applications at Regional Scale, IFREMER) (Lazure and Dumas, 2008). The high resolution MARS3D-RHOMA model configuration (From RHOne River to MArseille Bay) was developed to better understand the anthropogenic impact and inputs of particulate and dissolved organic matter of the Marseille metropolis, the emissaries, the coastal rivers, and the Rhone River.

The hydrodynamic MARS3D-RHOMA model configuration evaluation was based on in situ hydro-meteorological data acquired in 2007 and 2008 (Pairaud et al., 2011) in the Rhone River and Marseille area. The MARS3D-RHOMA configuration used a realistic bathymetry, a discretization grid with a resolution of 400 m in the horitontal plane and 30 vertical layers and solved the hydrodynamical and dispersion equations with a time step of 30 seconds. The model is forced by the WRF atmospheric model (Yohia, 2017), the Rhone River daily flow, the urban creek flows (Huveaune and Aygalades), the Cortiou's wastewater outputs, precipitations, and atmospheric factors (*e.g.* winds). The western and southern open boundaries are forced by the larger MARS3D-MENOR configuration (north-western Mediterranean MARS3D area - 1.2 km resolution) (Nicolle et al., 2009; Garnier et al., 2014). The model and the meteorological factors were updated to simulate the year 2020.

The MARS3D-RHOMA simulations were run for February 2020 and September 2020 during one month before our sampling campaign. The outputs (simulation results of currents, temperature, and density) were implemented to drive the Ichthyop software (Lett et al., 2008) and simulate the Lagrangian dispersion of MPs. In the Ichthyop software, 3000 particles (corresponding to the total found in the bay of Marseille) were released from potential source locations of MPs. MP particles were considered to have a mean size of 350 μm and were assumed to be floating. Biologic processes were not considered.

2.6. Statistical analysis

The statistical analysis of MP concentrations in water and sediments used a nonparametric test, because of the small number of stations and samples and the non-gaussian distribution of the data. Consequently, the Kruskal-Wallis test associated with the Dunn test at 95% confidence level was chosen. The difference in the MP abundance between the southern Bay and the northern Bay, as well as the spatial and temporal differences and typology variations, were tested with the Kruskal-Wallis test associated with the Dunn test. The mean value between the replicates for each station and the standard deviation for each sample were calculated. All analyses were conducted using the GraphPad Prism 8 and Excel software.

3. Results

3.1. Blanks and contamination

Water blanks (n=10) contained 1.5 ± 0.7 MP, mainly transparent fibres and spherical white fragments. Their size varied from 1 mm for the fibres to 0.5 mm for the fragments. They were similar to those observed in surface water samples. Sediment blanks (n=8) contained 32 ± 22.6 MP, mainly 95.3% fibres and a few films (4.7%), of various colours. Most of these MPs resembled those observed in sediment samples. It is likely that high MP concentrations in sediment blanks could be derived from the conditioning of the diatom earth (plastic container) and the longer protocol process time. The filtered distilled water used for all the experimentations and on the vessel contained 0 ± 1 MP. Field airborne contamination can be considered as negligible with 0.7 ± 1.2 MP (n=11). Most aerial contamination consisted of non-plastic fibres (98.6% of cotton and plant fibres). In the following results, MP concentrations are given corrected from blank values by removing the blank MP number from the MP counting.

3.2. MPs in surface water

3.2.1. Microplastics abundance

MPs were detected at every station for each campaign (Fig. 2A). Generally, the southern Bay displayed higher concentrations (mean 7.00 ± 16.54 MP.m^{-3}) than the northern Bay (mean 4.83±7.17 MP.m^{-3}), but the difference was not significant (p-value=0.480) (Table. S2). In surface water the mean MP abundance was 5.79 ± 12.7 MP.m^{-3}. The minimum MP concentration was 0.47 ± 0.09 MP.m^{-3} (RN3, March 2021) while the maximum MP concentration was 72.66 ± 18.16 MP.m^{-3} (RN2, February 2020).

Variability through time was observed. MP concentrations were significantly higher in February 2020 at all stations than for other seasons (Fig. 2A). Overall, MP concentrations in September 2020, March and September 2021, and March 2022 were very similar. Even though MP concentrations in September 2020 seemed higher than those of March 2021, September 2021, and March 2022, they were far lower than those of February 2020 (Fig. 2A). The graphical trend showing abnormal MP concentrations in February 2020 was confirmed by statistical analysis with February 2020 being significantly different from March and September 2021 and March 2022 ($p<0.005$) (Table. S1) and to a lesser extent different from September 2020 ($p<0.05$). Furthermore, seasonally, there were no statistical differences between spring and autumn (p-value = 0.804).

Regardless of the statistical test results, temporal variations punctually occurred. Considering an average value for all stations, the MP concentration in February 2020 (22.74 ± 23.60 MP.m^{-3}) was higher than in September 2020 (4.09 ± 2.09 MP.m^{-3}), March 2021 (1.57 ± 0.64 MP.m^{-3}), September 2021 (1.99 ± 1.19 MP.m^{-3}) and March 2022 (and 1.69±0.61 MP.m^{-3}). Regardless of the season, an average MP concentration of 5.79 ± 12.7 MP.m^{-3} was measured in the surface waters of the Bay of Marseille.

3.2.2. MP Typology and chemical characterisation

For all water samples, fibres (mostly transparent) were the most abundant MP type representing 66.9–88.7% (Fig. 3A). Fragments were the second most common type of MP (8.4 – 29.4%), with foam (2.3 – 8.1%) and film (0.6 – 2.6%) being poorly represented. However, punctual heterogeneity occurred as in March 2021 where RN1, RS1, and RS3 stations displayed 50% of fragments whereas sample RN3 had >60% of foams (Fig. S2).

The most striking feature in the MP distribution in the bay of Marseille is that, over the four seasons and across the seven stations sampled, the 1 mm-sized MPs dominated with an average occurrence of 27%

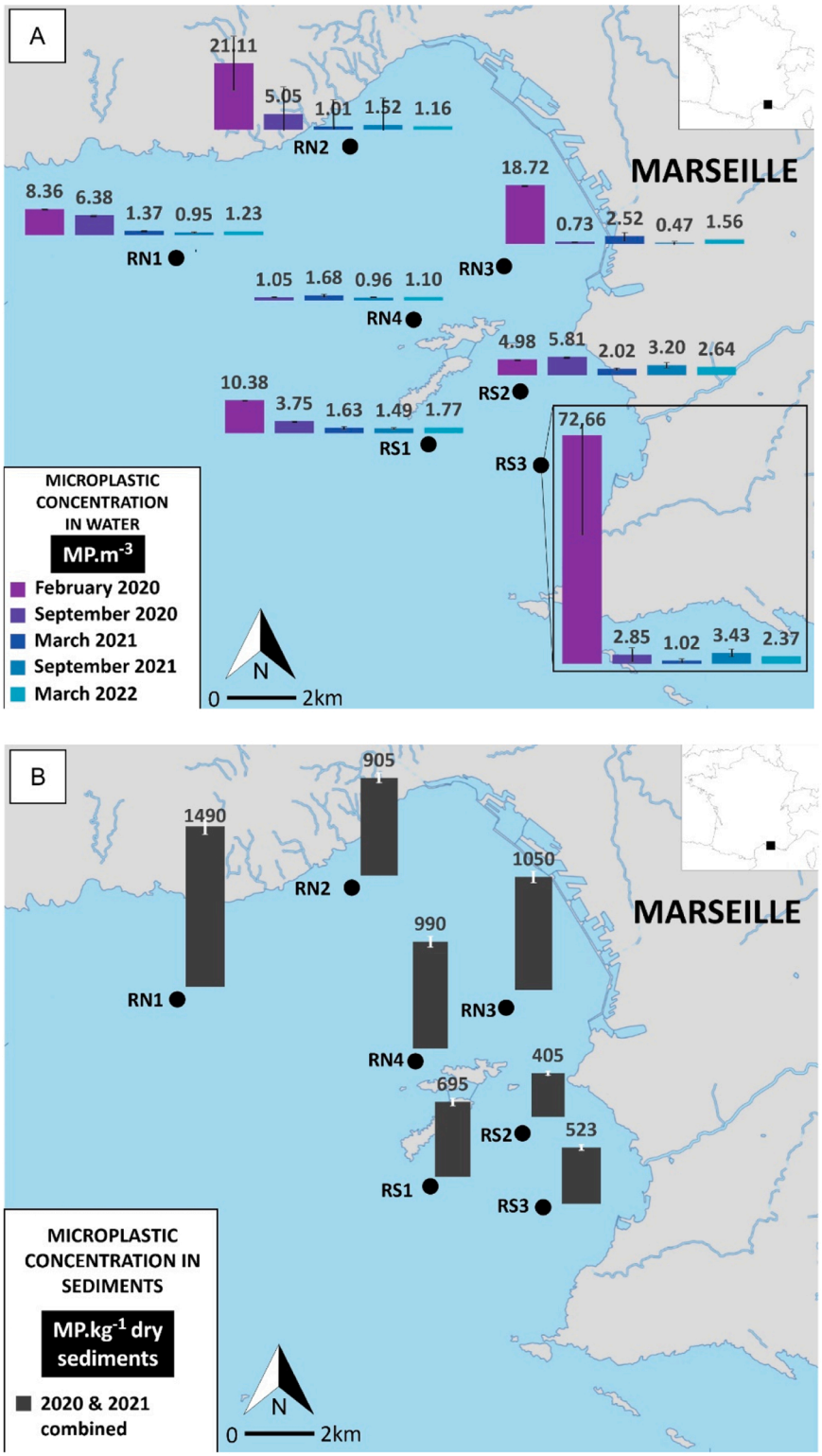

Fig. 2. (A) Microplastic concentration (MP.m^{-3}) in surface water samples (February 2020, September 2020, March 2021, September 2021, March 2022) in the Bay of Marseille. (B) Microplastic concentration (MP.kg^{-1} dw) in sediment samples in the Bay of Marseille. Error bars are indicated in black (A), and in white (B).

(Fig. 3B) and 75.1% of particles observed sized between 250 μm and 1 mm. The second most abundant size class was 0.5 mm-sized MPs with an average occurrence of 19%. Interestingly, about 20% of MPs were <0.25 mm in February and September 2020, whereas in March and September 2021 and March 2022, they accounted for <10%.

Among the particles analysed by ATR-FTIR (n= 50), 55% were chemically identified as plastic belonging to seven polymer types (Fig. 3E). The most abundant polymer was polypropylene (PP – 21.9%), followed by polyethylene (PE – 18.1%), polyamide (nylon, PA – 3.8%), polyvinyl chloride (PVC – 3.8%), polystyrene (PS – 2.9%), polyvinyl siloxane (PVS – 1.9%), polyurethane (PU – 1.9%) and finally, polyvinyl acetate (PVAc – 0.9%).

The 45% of remaining particles (mainly foams and fragments) that were not identified as MPs did not correspond to any spectra of the

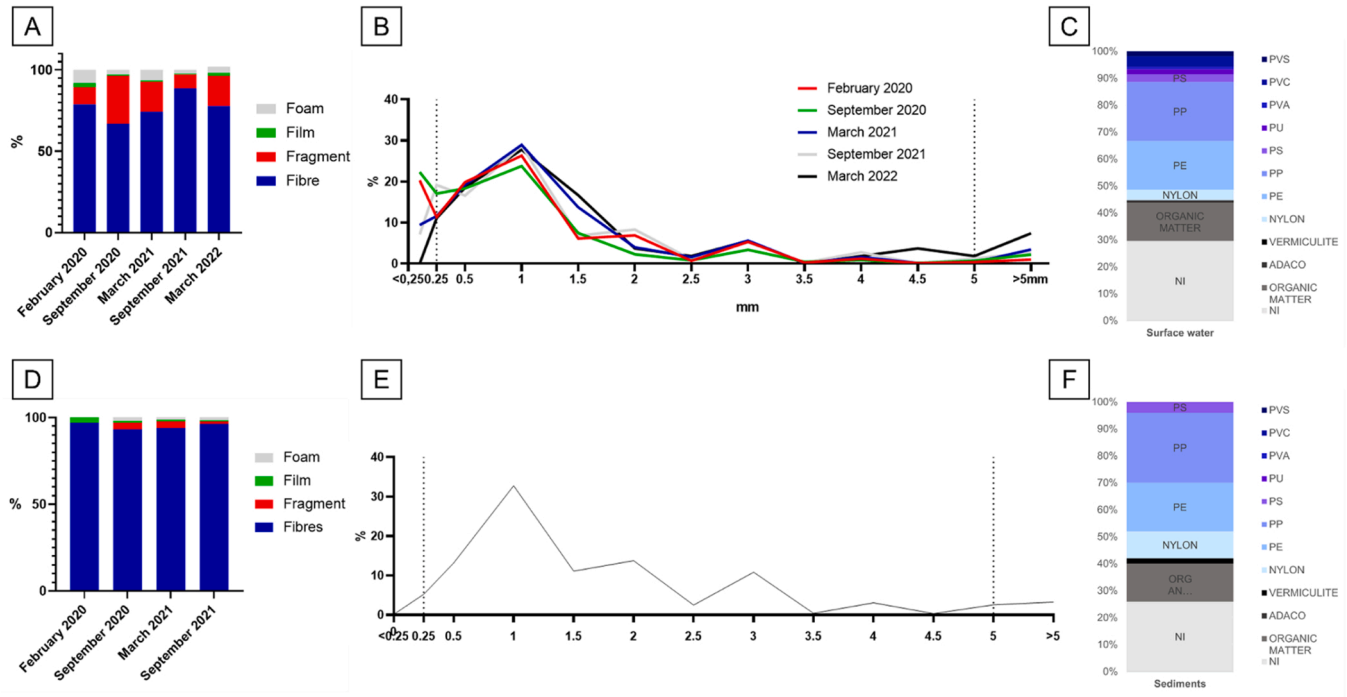

Fig. 3. MP typology and chemical characterization of surface water and sediment samples. (A) Surface water microplastic typology; (B) Surface water microplastics size distribution.; (C) Water surface particles chemical type; (D) Sediment microplastic typology; (E) Sediment microplastic size distribution; (F) Sediment particles chemical types. For panels B and E, the dotted lines indicate the sieve mesh size used for sample preparation.

databases (NI – 29.5%) or were identified as non-plastic particles such as organic matter (14.3%) or minerals (0.9%).

3.3. MPs in bottom sediments

3.3.1. Microplastics abundance

Similarly to water samples, MPs were detected in all bottom sediment samples (Fig. 2B). MP concentrations varied from 405 ± 106 MP. kg^{-1} dw (RS2) to 1490 ± 127 MP.kg^{-1} dw (RN1) (Fig. 2B). Since there were no statistical differences between spring and autumn (Table. S2), MP concentrations were averaged at each site for all the sampling periods. Graphically, high MP concentrations were recorded in the northern bay with values ranging from 905 to 1490 MP.kg^{-1} dw. The southern bay displayed lower concentrations ranging from 405 to 990 MP. kg^{-1} dw.

All sites combined, sediments from the bay Marseille contained in average 856 ± 412 MP. kg^{-1} dw.

3.3.2. MP typology and chemical characterisation

All stations combined, >95% of MPs found in sediments were fibres (Fig. 3C), a feature that is more pronounced than in water samples. Fragments, film, and foam accounted for <2%. A similar trend to that of water samples was observed with MP size distribution in sediment samples. All seasons combined, over the seven sites, >30% of MPs were in the 1 mm size range (Fig. 3D) sometimes reaching >50% as in sample RS2. RS3 was the only site where 37.25% of MPs were in the size class of 0.5 mm. Among the particles analysed by ATR-FTIR, 58% were identified as plastic belonging to four polymer types (Fig. 3E). The most abundant polymer was PP (26%), followed by PE (18%), PA (10%), and PS (4%). The 42% of remaining particles that were not identified as MP did not correspond with any spectra of the databases (NI – 26%) or were identified as non-plastic particles such as organic matter (14%) or minerals (vermiculite – 2%).

4. Discussion

4.1. MP distribution in the bay of Marseille

4.1.1. Surface water

The mean surface water MP concentration (5.79 ± 12.7 MP.m^{-3} or 9.1 10^5 ± 1.3 10^6 MP.km^{-2}) reported in the Bay of Marseille between 2020 and 2022 exhibited the same magnitude as the MP abundance recorded over a decade by several studies (Collignon et al., 2012; Gérigny et al., 2022; Ourgaud et al., 2022; Schmidt et al., 2018, 2021; Tsiaras et al., 2022) (Fig. 4A).

Direct inter-study comparison can be challenged by different sampling methodologies and extraction protocols. In all the above-mentioned studies, the mesh size of the manta net was 330 μm or 333 μm and plastic items ≤5 mm were considered. Two protocols were used for sample preparation: either without treatment (direct sieving and filtration, gravity separation from organic matter) (Gérigny et al., 2022; Collignon et al., 2012), or with treatment (oxidation and densimetric separation) (Ourgaud et al., 2023; Tsiaras et al. 2022). For example, the protocol used in Schmidt et al. (2018) removed all the fibres in their counts to avoid any contamination risks. When fibres are removed from our counts, the results obtained are close to the estimations of Schmidt et al. (2018) (Fig. 4A). In Gérigny et al. (2022), the extraction protocol used a densimetric separation step and no oxidation. We have however shown that neither densimetric separation nor the oxidation step alter the number of MPs extracted (Fig. S1). Additionally, all our reagents were filtered for analysis.

Therefore, we suggest that all the studies considered here provide comparable results. Most of the MP concentrations fall in the same range of values (1.0 10^6 MP.km^{-2}). Two exceptions can be mentioned, with abundance peaks observed in the Bay in June 2018 (1.8 10^6 MP.km^{-2}, Gérigny et al., 2022) and in February 2020 (2.5 10^6 MP.km^{-2} mean value, our study, Fig. 4A). Apart from these isolated values, the absence of general spatial or temporal trends in the Bay since 2010 is revealed despite the highly variable dynamics at a local scale (Fig. 4A).

Our results are coherent with data from semi-enclosed bays even if

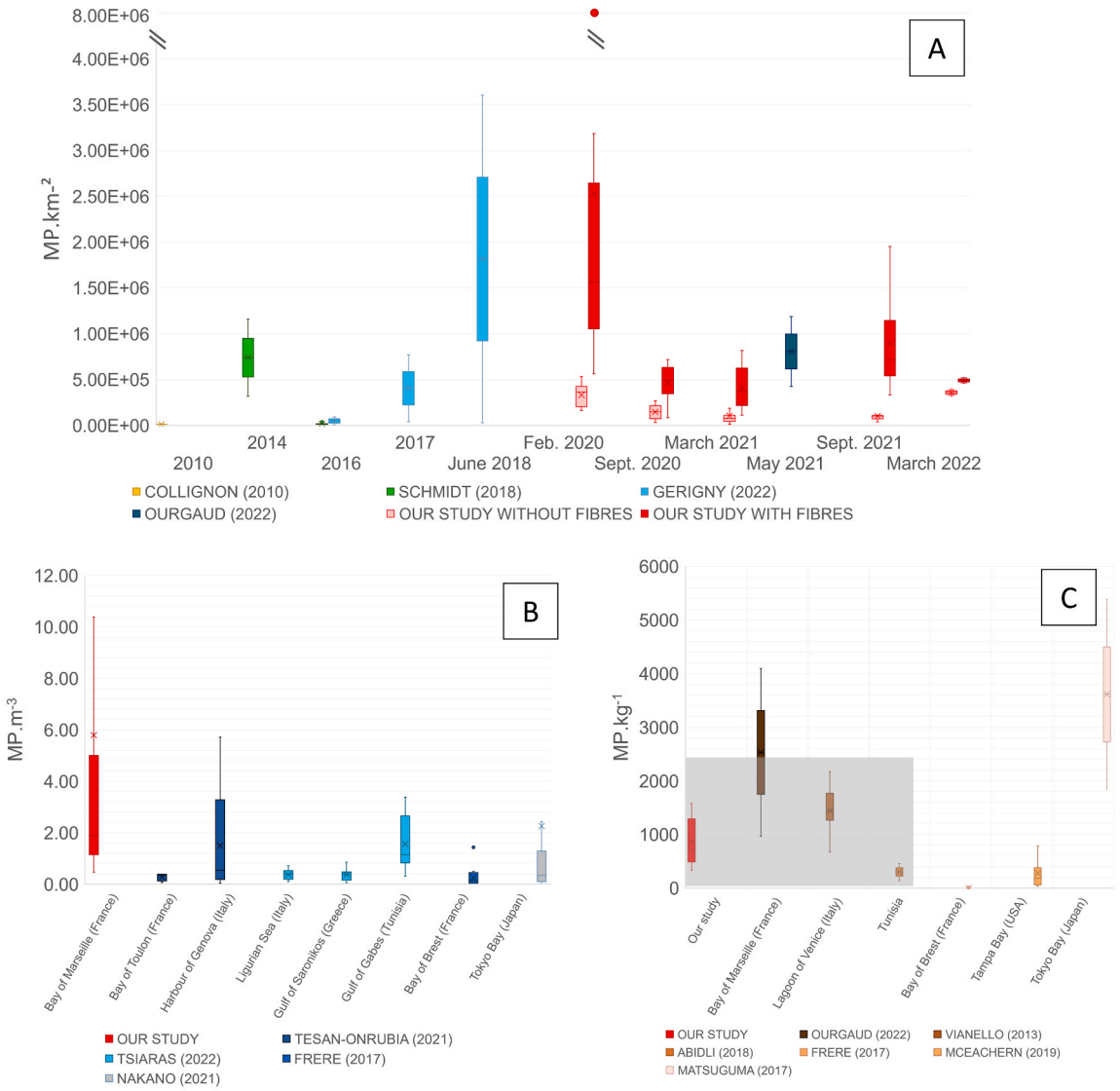

Fig. 4. (A) Comparison of the mean water MP concentration (MP.km^{-2}) in the Bay of Marseille from Collignon et al., 2012; Gérigny et al., 2022; Ourgaud et al., 2022; Schmidt et al., 2018, 2021; Tsiaras et al., 2022 and this study. (B) Comparison of the mean water MP concentration (MP.m^{-3}) in Mediterranean (Tesan-Onrubia et al., 2021, Tsiaras et al., 2022) and non-Mediterranean (Frère et al., 2017, Nakano et al., 2021) semi-enclosed bay systems similar to the Bay of Marseille (Tesan-Onrubia et al., 2021, Tsiaras et al., 2022). (C) Comparison of the mean sediment MP concentration (MP.kg^{-1} dry sediment) between 6 studies in Mediterranean (Ourgaud et al., 2022, Vianello et al., 2013, Abidli et al., 2018) and international (Frère et al., 2017, McEachern et al., 2019, Matsuguma et al., 2017) semi-enclosed bay systems similar to the Bay of Marseille. The grey zone represents the range of MP abundance noticed in the Mediterranean marine sediments (min. 1.66 ± 1.77 MP. kg^{-1}; max. 2.43·10^3 ± 2·10^3 MP; kg^{-1}; Simon-Sanchez et al., 2022a). For (A),(B), (C), the box plots are limited by the Q1 and Q3 (quartiles), showing the mean value (cross) and the median value (horizontal bar). The vertical bars indicate the total range of MP concentration. In panel (A) the absolute MP value for RS3 (February 2020) is not shown on real scale for graphical reasons but is included in the statistical calculations.

the Bay of Marseille appears to be more contaminated than other French bays (Fig. 4B). The mean MP concentration of 5.79 ± 12.7 MP.m^{-3} in the Bay of Marseille (this study) is higher than values recorded in the Mediterranean Sea and in French bays: 0.439 MP.m^{-3} in the Gulf of Saronikos (Greece) (Tsiaras et al., 2022), 1.564 MP.m^{-3} in the Gulf of Gabes (Tunisia, Tsiaras et al., 2022), 1.49 MP.m^{-3} in the Bay of Genova (Italy; Tesán Onrubia et al., 2021), 0.28 MP.m^{-3} in the Bay of Toulon (France; Tesán Onrubia et al., 2021), and 0.25 MP.m^{-3} in the Bay of Brest (France; Frère et al., 2017) (Fig. 4B).

When compared to Asian bays, MP concentrations in the Bay of Marseille also displayed higher values: 2.26 MP.m^{-3}, in Tokyo Bay, Japan (Nakano et al., 2021), and 0.4 MP.m^{-3} in Cua Luc Bay to 28.4 MP. m^{-3} in Dinh estuary, in Vietnam (Strady et al., 2021).

Our results add to the global picture of surface water plastic pollution. Recent work by Chevalier et al. (2023) suggests that surface water pollution might be underestimated since the water column contamination is not taken in account. In the Bay of Marseille, it was possible to estimate MP distribution in the sub-surface water from surface concentration data when considering environmental parameters (*e.g.* wind conditions) (Chevalier et al., 2023). This site-specific approach needs however to be completed by other in-situ data, to improve MP distribution control forcing in the water column and the potential accumulation of MPs in the sedimentary compartment. Even if the comparison must be considered with caution because of the different methodologies in sampling, extraction and identification, the compilation of results in the Bay of Marseille showed a constant level of contamination despite the implementation of a zero plastic waste policy since 2016 by regional authorities. It is clear that, actions against plastic waste should be implemented at a larger scale in the Mediterranean Sea to reduce the level of microplastic contamination (Ziveri et al., 2023). Once more this

emphasises the importance of field data as a valuable diagnostic tool of contamination in coastal areas for decision makers.

4.1.2. Sediments

To our knowledge, our study provides the first extended dataset on sediment MP contamination at 7 sites in the bay of Marseille, in addition to discrete quantification by Ourgaud et al. (2022) at 2 sites south of Frioul Islands and offshore, respectively. Here we report a mean MP concentration of 856 ± 413 MP.kg^{-1} dw whereas Ourgaud et al. (2022) recorded an average value of 2531 ± 1565 MP.kg^{-1} ww (Fig. 4C). However, different normalisation protocols (MP concentrations expressed as items per dry weight sediment versus wet weight) hinder direct comparison. Overall, we assume that both studies recorded comparable levels of contamination, within the range of values observed in other Mediterranean sediments (Fig. 4C). It should, however, be pointed out that the basin-wide concentration range is large. This variability is even more pronounced when considering areas with specific forcings outside the Mediterranean Sea (e.g., tide range, urban pressure) (McEachern et al., 2019; Matsuguma et al., 2017; Frère et al., 2017) (Fig. 4C), highlighting the influence of contrasted hydrodynamic and anthropic contexts on MP accumulation processes in sediments.

In the Bay of Marseille, no significant differences in MP concentrations were revealed between stations despite contrasted grain-size distributions (Jeudy de Grissac and Le Fur, 1983; Vousdoukas et al., 2011). Some studies showed that MPs tend to preferentially accumulate in fine sediments related to low-dynamic areas (Strand et al., 2013; Vianello et al., 2013). However, other studies suggest that no clear trend can be established between sediment grain-size and MP deposition (*e.g.,* Alomar et al., 2018; Brown et al., 2010). We hypothesise that in the Bay of Marseille, MPs might accumulate preferentially in fine sediments from the northern Bay by contrast to the coarser-grained sediments from the southern Bay - a trend observed in our data but not statistically confirmed. Interestingly, the physico-chemical characteristics of the MPs (size, types, polymers) are comparable in water and sediment samples.

Low density MPs were found in sediment samples (e.g., PP, PS), raising the question of the biological and physical processes driving the surface-bottom coupling as well as the vertical transport in the water column of these compounds (e.g., biofouling, incorporation into organic matrices, advection) (*e.g.*, Harris, 2020). Furthermore, the dominance of small-sized (~1 mm) MPs in surface water and sediment suggests a low contribution of offshore input in the Bay, as larger MPs are expected to travel long distances in the open sea (Schmidt et al., 2018; Tsiaras et al., 2022).

4.1.3. Fibre typology and characterisation

The type and size distribution observed in our samples, with fibres being dominant, is commonly observed in the north-western Mediterranean Sea (Santini et al., 2022).

The MPs observed in the Bay of Marseille are relatively small (0.3–1 mm) (Fig. 2B, E) and have the same size range as that found in previous studies on the Bay (Gérigny et al., 2022; Schmidt et al., 2018). This is also in full agreement with data observed in the Mediterranean Sea showing that 50% of microfibres have a length <2 mm (33% between 1 mm and 2 mm) (Santini et al., 2022).

The size of the MPs may be used as an indicator of the distance of the MP from its source with larger particles near the source and fragmented and smaller MP far from the source (Frias et al., 2014). Based on this hypothesis, our data suggest four scenarii: (i) MPs entering the Bay of Marseille are distant from the source, (ii) the MPs released by the urban areas are negligible, (iii) the MPs released by the urban areas are rapidly expelled outside the Bay, or (iv) the small MPs (mostly fibres) are directly released by wastewater treatment plant outputs Additional data from outside the Bay are required, however, to elucidate these issues.

In our water samples, fibres represented almost 77.2% of the microlitter. The fragments derived from the breakdown of microplastic litter (secondary MPs) accounted for 16.7%. Foams (4.9%) and films (1.2%) were the least abundant types in the surface water despite their low density and their high buoyancy. This distribution could be linked either to their ability to be dispersed vertically or to a lower input of these types in the Bay.

Various sources can promote the delivery of these particles in surface waters: clothes laundering and its release though wastewater facilities, or the degradation of fishing supplies such as nets or fishing lines. In the Bay of Marseille, the Cortiou WWTP or the Rhone River are known for their high MP contamination (Schmidt et al., 2018) and could explain the dominance of fibres in the samples. This local signature is also in accordance with other studies on the Mediterranean Sea where fibres accounted for 47% of the MPs encountered (Santini et al., 2022). According to several studies, the Mediterranean Sea is the most fibre-contaminated marine basin (Constant et al., 2020; Suaria et al., 2016). We found however some discrepancies with MP typology observed in previous studies on the Bay of Marseille which reported the dominance of fragments in the Bay (Gérigny et al., 2022), whereas in our samples fibres are dominant. The MP abundances are similar in the two studies (Gérigny et al., 2022, our study, Section 4.1.1.) but the type distribution differs. In Gerigny et al. (2022) fibres are present (accounting for 24–72%) but are mostly reported as mesoplastics (plastic particles with a size range of 5 – 20 mm). Between 2016 and 2018, the most frequently encountered MP type was fragments in the bay of Marseille (Gérigny et al., 2022) and from 2020 to 2022 (this study) the most abundant type found was fibres. The different methods used in the studies could be one reason for the shift in type distribution. Another explanation could be linked to a change of MP sources in the Bay of Marseille.

4.2. Hydrometeorological controls on MP distribution

4.2.1. Main hydrodynamic factors

The Bay of Marseille is known to have highly variable hydrometeorological conditions strongly influenced by NW (Mistral) and SE wind regimes, controlling up/downwelling events. Mediterranean rainfalls are scarce but can be intense. Surface water is changeable, eddies and currents can be created episodically, and the Northern Current (part of general circulation in the NW Mediterranean Sea) can enter the bay under certain wind conditions. The impact of this hydrodynamical context on particle dispersion was examined using high resolution modelling based on the MARS3D-RHOMA model (Fraysse et al., 2013, 2014; Millet et al., 2018; Ross et al., 2016; Schmidt et al., 2019; Chevalier et al., 2023). These studies have highlighted four dominants hydrodynamic forcings to explain particle dispersion in the Bay of Marseille:

- The NW wind (Mistral) and the SE winds dominating the bay, intimately linked to the surface water fluxes induced by the swell. The winds, swell and short-lived surface currents can evict or transport particles depending on their direction and strength.
- Precipitations and the associated runoff bringing land and urban litter. In addition, the flow of the urban creeks (Aygalades and Huveaune) can contribute after heavy rain events (AGAM 2016, EPAGE HUCA). The Huveaune, normally flowing into the Cortiou Calanque, can be deviated towards its natural course and discharge directly into the Bay of Marseille (if the flow >30 m3.s-1).
- The northern current, which can intrude the Bay of Marseille and transport particles from the Cortiou wastewater outlet (Millet et al., 2018)
- The Rhone River plume can be advected towards the Bay of Marseille linked to wind shifts episodes.

All these conditions may result in the mean MP distributions observed in the Bay of Marseille during our sampling period (2020–2022) and also in earlier surveys (Collignon et al., 2012; Gérigny

et al., 2022; Ourgaud et al., 2022; Schmidt et al., 2018, 2021; Tsiaras et al., 2022).

However, one specific period emerged in our data: the high MP content observed in all stations in the Bay of Marseille for February 2020, despite the fact that neither the Northern Current nor swell and runoff were dominant factors at this period. February 2020 is characterised by an intense NW-E wind regime followed by a SE wind regime with several wind shifts (16th, 20th February and 24th February) less than one week before our sampling (25th and 27th February 2020) (Fig. S3). These wind shifts could have favoured the formation of the Marseille Eddy and consequently the plume intrusion (Fraysse et al., 2014). Indeed, the MARS3D-RHOMA simulation for February 2020 showed that Rhone plume intrusions occurred at least 4 times during this period: (i) 3rd of February (measured in-situ, Chevalier et al., 2023); (ii) 10–11th of February; (iii) 13–17th of February; (iv) 22–23rd of February (Fig. 5; Fig S4A). This is an unusual number of Rhone plume intrusions during such a short period. Following Fraysse et al.,(2014), the intrusion events (i) and (iii) correspond to the "short-lived" event (large spatial coverage and short duration) whereas the intrusion event (ii) is categorised as a "big" event (large spatial coverage and long duration).

The particularity of these conditions is obvious when they are compared with the situation in September 2020, where no Rhone plume intrusions were reported with the MARS3D-RHOMA simulation (Fig. S4B).

The Ichthyop dispersion model for the same period was used to simulate the MP drift during the 13–17th February intrusion event. About 3000 particles were released on 15th February 2020 from the Rhone delta area and tracked until the sampling date (25th February). The beginning of the simulation showed an eastward transport of some of the particles toward the bay of Marseille (Fig. 6A) by contrast to a southward transport during a Mistral event (Fig. 6B) or a westward transport during typical outflow conditions. The eastward drift of the particles is maintained by the formation of the Marseille Eddy (Figs. 5C, 6C), linked to the third intrusion event (22nd February), which promoted the transport of the particles in the bay of Marseille (Fig. 6D).

We suggest that these successive Rhone plume intrusions during February 2020 contributed to the transport of plastic contamination into the Bay, thus explaining the high MP concentrations for this period. Large European rivers are important pathways for land-derived plastic litter to coastal areas (Castro-Jiménez et al., 2019). The riverine system contributes significantly to marine MP contamination since 1.15–2.41 million tonnes of plastics are discharged annually from the rivers into the ocean (Lebreton et al., 2017). The Mediterranean Sea is also impacted by the polluted river fluxes with approximately 223,000 macroplastic items being annually transported by the Rhone to the Gulf of Lion (Castro-Jiménez et al., 2019). The MP flux estimation ranges between 73 kg to 7.78 t transported annually by the Rhone to the Gulf of Lion (Schmidt et al., 2019).

Our MP data obtained from a three-year survey documented the influence of episodic Rhone intrusions that impacted the MP contamination at the scale of the Bay of Marseille. This study highlights the need to perform a regular monitoring to capture fine scale forcing factors on MP distribution in coastal areas. These circumstances do not rule out the other hydrometeorological and anthropogenic factors operating since previous studies have highlighted the direct impact of the Cortiou WWTP and direct urban pressure (Gérigny et al., 2022; Tsiaras et al., 2022).

4.2.2. *Direct urban pressure*

Marseille is an attractive tourist city under strong demographic pressure, especially during the summer months, inducing a factor of pollution and contamination. Several human activities can lead to the release of MPs in the Bay of Marseille. The harbour activity (commercial and touristic) represents an important perennial source for MP contamination in the Bay of Marseille. In addition, waste dumping in the city or directly in the marine bay also results in a significant input of plastic litter. The litter phenomenon is most probably increased during summer, linked to beach occupation, swimming, boating, water sports, as well as fishing nets. At this stage, it is difficult to differentiate between the different types of input and sources related to these activities. However, the impact of tourist activities on the MP contamination of the Bay of Marseille cannot be assessed from our results since no significant change was observed before (February) and after (September) the summer tourist season. In addition, it is interesting to notice that the Covid-19 crisis did not impact MP concentration in the bay, with no

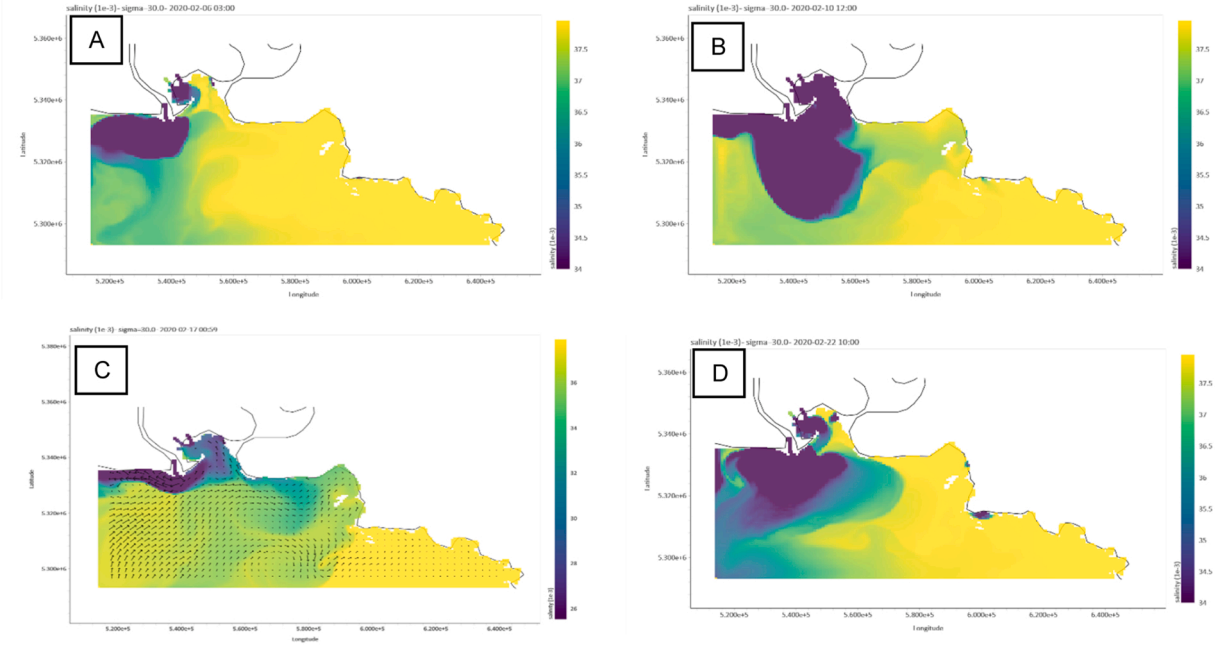

Fig. 5. Modelled surface salinity simulations (Model MARS3D-RHOMA) showing (A) typical outflow conditions (no intrusion, 6th of February 2020), (B)"short-lived" intrusion event (10th of February 2020), (C) "big" intrusion event (13th-17th of February 2020) with the arrows representing the surface currents and highlighting here the formation of the Marseille Eddy, and (D)"short-lived" intrusion event (22nd of February 2020).

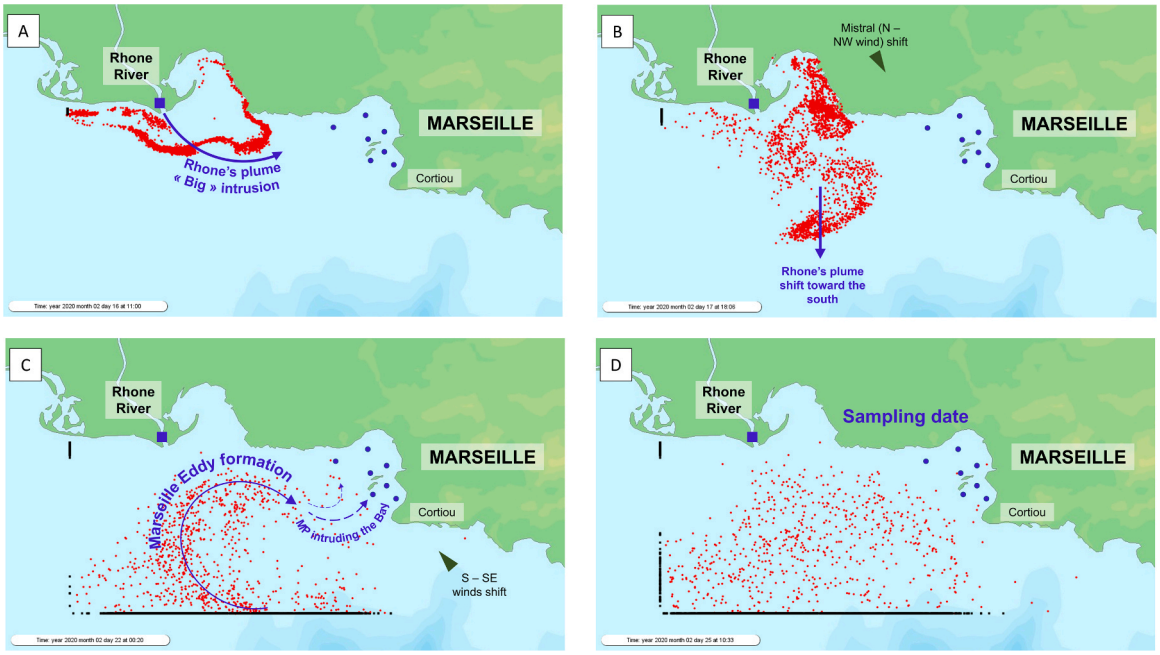

Fig. 6. Simulated plastic particle dispersion between 15/02/2020 (beginning of the Rhone River plume "big" intrusion event) and 25/02/2020 (sampling date in the Bay of Marseille, sampling stations are represented by the blue squares). 3000 particles released from the Rhone River mouth (blue square) dispersed within the model MARS3D-RHOMA boundaries. (A) 16/02/2020: the particles released from the Rhone River move eastwards, advected by the plume. (B) 17/02/2020: the plume intrusion event ends by a destruction mechanism of Mistral (NW wind) and the particles move southward, pushed by the Mistral wind. (C) 22/02/2020: the wind shift (N-NW to S-SE) favoured the formation of the Marseille Eddy and another plume intrusion event occurs. The particles are remobilized and are dispersed toward the Bay of Marseille. (D) 25/02/2020: sampling date. Some of the particles released the 15/02/2020 from the Rhone River enter the Bay and are located in the vicinity of the sampling stations.

increase in MP concentration after the return of tourist and cruise activities in 2021. However, the collected data are not sufficient to precisely quantify the diversity of anthropogenic sources in the bay of Marseille (*e.g.* those linked to the bay activity versus those related to waste management).

5. Conclusion

Spatio-temporal variability of MP contamination in the Bay of Marseille was investigated in surface water and sediment samples collected over 3 years (2020–2022) during 5 seasonal campaigns. The hydrodynamical circulation model MARS3D-RHOMA was used with in-situ data to test the influence of meteorological and hydrodynamic features on the concentration of MPs during the study period. Our results provided a complete data set of MP distribution, abundance, size, and types for 50 samples. Data were obtained using an optimised - quick and eco-friendly - protocol validated for the study area. MP average concentrations in surface water matched well quantitative estimates reported in the Bay since 2012 and confirmed a constant level of contamination over a decade in the Bay of Marseille. Furthermore, we provide the first dataset of MP concentration in sediments for the bay. The physico-chemical characteristics of MPs (colour, size, types, polymers) are similar in water and sediment, raising the question of the processes driving the transport of these low-density particles through the water column. The influence of the Rhone intrusion as a source of MPs in the bay was documented using the high-resolution model MARS3D-RHOMA and the Ichthyop Lagrangian dispersion model for an abnormal high-concentration event such as those reported in February 2020. Our study captured an exceptional hydrodynamic event characterised by a succession of Rhone plume intrusions impacting the MP distribution and contamination in the Bay of Marseille. These results emphasise the need to perform regular field monitoring combined with high resolution modelling to capture fine-scale events in complex hydrodynamic coastal areas.

CRediT authorship contribution statement

A. Alcaïno: formal analysis, investigation, methodology, visualization, writing (original draft, review & editing); **L. Vidal:** conceptualization, investigation, methodology, visualization, writing (original draft, review & editing), funding acquisition; **L. Licari:** conceptualization, investigation, methodology, visualization, writing (original draft, review & editing); **C. Paillès:** investigation, methodology, writing (original draft, review & editing); **S. Conrod:** formal analysis, methodology; **J. Dauvier:** formal analysis, methodology; **C. Chevalier:** investigation, methodology, visualization, writing (original draft, review & editing); **C. Pinazo:** investigation, methodology, visualization, writing (original draft, review & editing); **M. Grelaud:** investigation, writing (original draft, review & editing); **P. Ziveri:** funding acquisition

Declaration of Competing Interest

The authors declare that they have no known competing financial interests or personal relationships that could have appeared to influence the work reported in this paper.

Data availability

I have shared the raw data as an excel file and provide them as "Supplementary data" in the Attach File step.

Acknowledgements

AA was funded by the PLASMA project supported by the research federation ECCOREV, the institute Carnot "Eau & Environnement" and the Fondation de la Mer. PZ and MG acknowledge the i-plastic project (JPI-Oceans—Grant PCI2020–112059) and the Generalitat de Catalunya (MERS, 2017 SGR-1588) for financial support. Amélie Pujol is acknowledged for her help in additional sample preparation and Vincent

Faure for his contribution for the model visualiser SimuXplorer. We would also like to thank Loïc Guilloux (MIO), the Service Atmosphère Mer (SAM, MIO), and the crew of the R/V Antédon II for technical assistance with sampling.

Appendix A. Supporting information

Supplementary data associated with this article can be found in the online version at doi:10.1016/j.rsma.2024.103457.

References

AGAM, Agence d'urbanisme de l'agglomération marseillaise, 2016. Bâtir un projet de territoire autour du littoral.⟨https://www.agam.org/⟩.

Allou, A., Forget, P., Devenon, J.-L., 2010. Submesoscale vortex structures at the entrance of the Gulf of Lions in the Northwestern Mediterranean Sea. Cont. Shelf Res. 30 (7), 724–732. https://doi.org/10.1016/j.csr.2010.01.006.

Barnes, D.K.A., 2002. Invasions by marine life on plastic debris. Article 6883 Nature 416 (6883). https://doi.org/10.1038/416808a.

Barrows, A.P.W., Neumann, C.A., Berger, M.L., Shaw, S.D., 2017. Grab vs. neuston tow net: a microplastic sampling performance comparison and possible advances in the field. Anal. Methods 9 (9), 1446–1453. https://doi.org/10.1039/C6AY02387H.

Castro-Jiménez, J., González-Fernández, D., Fornier, M., Schmidt, N., Sempéré, R., 2019. Macro-litter in surface waters from the Rhone River: plastic pollution and loading to the NW Mediterranean Sea. Mar. Pollut. Bull. 146, 60–66. https://doi.org/10.1016/j.marpolbul.2019.05.067.

Chevalier, C., Vandenberghe, M., Pagano, M., Pellet, I., Pinazo, C., Tesán Onrubia, J.A., Guilloux, L., Carlotti, F., 2023. Investigation of dynamic change in microplastics vertical distribution patterns: the seasonal effect on vertical distribution. Mar. Pollut. Bull. 189, 114674 https://doi.org/10.1016/j.marpolbul.2023.114674.

Cincinelli, A., Martellini, T., Guerranti, C., Scopetani, C., Chelazzi, D., Giarrizzo, T., 2019. A potpourri of microplastics in the sea surface and water column of the Mediterranean Sea. TrAC Trends Anal. Chem. 110, 321–326. https://doi.org/10.1016/j.trac.2018.10.026.

Collignon, A., Hecq, J.-H., Glagani, F., Voisin, P., Collard, F., Goffart, A., 2012. Neustonic microplastic and zooplankton in the North Western Mediterranean Sea. Mar. Pollut. Bull. 64 (4), 861–864. https://doi.org/10.1016/j.marpolbul.2012.01.011.

Constant, M., Ludwig, W., Kerhervé, P., Sola, J., Charrière, B., Sanchez-Vidal, A., Canals, M., Heussner, S., 2020. Microplastic fluxes in a large and a small Mediterranean river catchments: the Têt and the Rhône, Northwestern Mediterranean Sea. Sci. Total Environ. 716, 136984 https://doi.org/10.1016/j.scitotenv.2020.136984.

Coyle, R., Hardiman, G., Driscoll, K.O., 2020. Microplastics in the marine environment: a review of their sources, distribution processes, uptake and exchange in ecosystems. Case Stud. Chem. Environ. Eng. 2, 100010 https://doi.org/10.1016/j.cscee.2020.100010.

Cózar, A., Sanz-Martín, M., Martí, E., González-Gordillo, J.I., Ubeda, B., Gálvez, J.Á., Irigoien, X., Duarte, C.M., 2015. Plastic accumulation in the Mediterranean Sea. PLOS ONE 10, e0121762. https://doi.org/10.1371/journal.pone.0121762.

Cutroneo, L., Reboa, A., Besio, G., Borgogno, F., Canesi, L., Canuto, S., Dara, M., Enrile, F., Forioso, I., Greco, G., Lenoble, V., Malatesta, A., Mounier, S., Petrillo, M., Rovetta, R., Stocchino, A., Tesan, J., Vagge, G., Capello, M., 2020. Microplastics in seawater: sampling strategies, laboratory methodologies, and identification techniques applied to port environment. Environ. Sci. Pollut. Res. 27 (9), 8938–8952. https://doi.org/10.1007/s11356-020-07783-8.

Demarcq, H., Wald, L., 1984. La dynamique superficielle du panache du Rhône d'après l'imagerie infrarouge satellitaire. Oceanol. Acta 7 (2), 159.

Eriksen, M., Lebreton, L.C.M., Carson, H.S., Thiel, M., Moore, C.J., Borerro, J.C., Galgani, F., Ryan, P.G., Reisser, J., 2014. Plastic Pollution in the World's Oceans: more than 5 trillion plastic pieces weighing over 250,000 Tons Afloat at Sea. PLOS ONE 9 (12), e111913. https://doi.org/10.1371/journal.pone.0111913.

Fabres, J., Kurvits, T., Nilsen, R., Pravettoni, R., & Agardy, T. (2012). State of the Mediterranean Marine and Coastal Envir-onment. https://doi.org/10.13140/RG.2.1.3013.2648.

Fraysse, M., Pairaud, I., Ross, O.N., Faure, V.M., Pinazo, C., 2014. Intrusion of Rhone River diluted water into the Bay of Marseille: generation processes and impacts on ecosystem functioning. J. Geophys. Res.: Oceans 119 (10), 6535–6556. https://doi.org/10.1002/2014JC010022.

Fraysse, M., Pinazo, C., Faure, V.M., Fuchs, R., Lazzari, P., Raimbault, P., Pairaud, I., 2013. Development of a 3D coupled physical-biogeochemical model for the Marseille Coastal Area (NW Mediterranean Sea): what complexity is required in the Coastal Zone? PLoS ONE 8 (12), e80012. https://doi.org/10.1371/journal.pone.0080012.

Frère, L., Paul-Pont, I., Rinnert, E., Petton, S., Jaffré, J., Bihannic, I., Soudant, P., Lambert, C., Huvet, A., 2017. Influence of environmental and anthropogenic factors on the composition, concentration and spatial distribution of microplastics: a case study of the Bay of Brest (Brittany, France). Environ. Pollut. 225, 211–222. https://doi.org/10.1016/j.envpol.2017.03.023.

Frias, J.P.G.L., Otero, V., Sobral, P., 2014. Evidence of microplastics in samples of zooplankton from Portuguese coastal waters. Mar. Environ. Res. 95, 89–95. https://doi.org/10.1016/j.marenvres.2014.01.001.

Galgani, F., Jaunet, S., Campillo, A., Guenegen, X., His, E., 1995. Distribution and abundance of debris on the continental shelf of the north-western Mediterranean Sea. Mar. Pollut. Bull. 30 (11), 713–717. https://doi.org/10.1016/0025-326X(95)00055-R.

Galgani, F., Leaute, J.P., Moguedet, P., Souplet, A., Verin, Y., Carpentier, A., Goraguer, H., Latrouite, D., Andral, B., Cadiou, Y., Mahe, J.C., Poulard, J.C., Nerisson, P., 2000. Litter on the Sea floor along European Coasts. Mar. Pollut. Bull. 40 (6), 516–527. https://doi.org/10.1016/S0025-326X(99)00234-9.

Galloway, T.S., Cole, M., Lewis, C., 2017. Interactions of microplastic debris throughout the marine ecosystem. Article 5 Nat. Ecol. Evol. 1 (5). https://doi.org/10.1038/s41559-017-0116.

Gatti, J., Petrenko, A., Devenon, J.-L., Leredde, Y., Ulses, C., 2006. The Rhone river dilution zone present in the northeastern shelf of the Gulf of Lion in December 2003. Cont. Shelf Res. 26 (15), 1794–1805. https://doi.org/10.1016/j.csr.2006.05.012.

Gérigny, O., Pedrotti, M.-L., El Rakwe, M., Brun, M., Pavec, M., Henry, M., Mazeas, F., Maury, J., Garreau, P., Galgani, F., 2022. Characterization of floating microplastic contamination in the bay of Marseille (French Mediterranean Sea) and its impact on zooplankton and mussels. Mar. Pollut. Bull. 175, 113353 https://doi.org/10.1016/j.marpolbul.2022.113353.

Harris, P.T., 2020. The fate of microplastic in marine sedimentary environments: a review and synthesis. Mar. Pollut. Bull. 158, 111398 https://doi.org/10.1016/j.marpolbul.2020.111398.

Henry, M., & Galgani, F. (2013, janvier 1). Observations des microplastiques sur les cotes francaises de mediterranee occidentale. 40ème Congrès de la CIESM. 28 octobre au 1er novembre 2013, Marseille. ⟨https://archimer.ifremer.fr/doc/00642/75436/⟩.

Hess, N.A., Ribic, C.A., Vining, I., 1999. Benthic Marine Debris, with an Emphasis on Fishery-Related Items, Surrounding Kodiak Island, Alaska, 1994–1996. Mar. Pollut. Bull. 38 (10), 885–890. https://doi.org/10.1016/S0025-326X(99)00087-9.

Jambeck, J.R., Geyer, R., Wilcox, C., Siegler, T.R., Perryman, M., Andrady, A., Narayan, R., Law, K.L., 2015. Plastic waste inputs from land into the ocean. Science 347 (6223), 768–771. https://doi.org/10.1126/science.1260352.

Jeudy de Grissac, A., Le Fur, C., 1983. Conditions de dépôt et nature sédimentaire des fonds de la rade Sud de Marseille avant les travaux d'aménagement de la plage du Prado. Ecol. Mediterr. 9 (1), 3–17. https://doi.org/10.3406/ecmed.1983.1014.

Kane, I.A., Clare, M.A., 2019. Dispersion, Accumulation, and the ultimate fate of microplastics in deep-marine environments: a review and future directions. Front. Earth Sci. 7. ⟨https://www.frontiersin.org/articles/10.3389/feart.2019.00080⟩.

Laist, D.W., 1987. Overview of the biological effects of lost and discarded plastic debris in the marine environment. Mar. Pollut. Bull. 18 (6), 319–326. https://doi.org/10.1016/S0025-326X(87)80019-X.

Lazure, P., Dumas, F., 2008. An external–internal mode coupling for a 3D hydrodynamical model for applications at regional scale (MARS). Adv. Water Resour. 31 (2), 233–250. https://doi.org/10.1016/j.advwatres.2007.06.010.

Lebreton, L.C.M., van der Zwet, J., Damsteeg, J.-W., Slat, B., Andrady, A., Reisser, J., 2017. River plastic emissions to the world's oceans. Nat. Commun. 8 (1), 15611 https://doi.org/10.1038/ncomms15611.

Lett, C., Verley, P., Mullon, C., Parada, C., Brochier, T., Penven, P., Blanke, B., 2008. A Lagrangian tool for modelling ichthyoplankton dynamics. Environ. Model. Softw. 23 (9), 1210–1214. https://doi.org/10.1016/j.envsoft.2008.02.005.

Masura, J., Baker, J., Foster, G., & Arthur, C. (2015). Laboratory Methods for the Analysis of Microplastics in the Marine Environment: Recommendations for quantifying synthetic particles in waters and sediments. [Report]. NOAA Marine Debris Division. https://doi.org/10.25607/OBP-604.

Mato, Y., Isobe, T., Takada, H., Kanehiro, H., Ohtake, C., Kaminuma, T., 2001. Plastic Resin Pellets as a transport medium for toxic chemicals in the marine environment. Environ. Sci. Technol. 35 (2), 318–324. https://doi.org/10.1021/es0010498.

Millet, B., Pinazo, C., Banaru, D., Pagès, R., Guiart, P., Pairaud, I., 2018. Unexpected spatial impact of treatment plant discharges induced by episodic hydrodynamic events: modelling Lagrangian transport of fine particles by Northern Current intrusions in the bays of Marseille (France). PLOS ONE 13 (4), e0195257. https://doi.org/10.1371/journal.pone.0195257.

Millot, C., 1990. The Gulf of Lions' hydrodynamics. Cont. Shelf Res. 10 (9), 885–894. https://doi.org/10.1016/0278-4343(90)90065-T.

Nakano, H., Arakawa, H., Tokai, T., 2021. Microplastics on the sea surface of the semi-closed Tokyo Bay. Mar. Pollut. Bull. 162, 111887 https://doi.org/10.1016/j.marpolbul.2020.111887.

Ourgaud, M., Phuong, N.N., Papillon, L., Panagiotopoulos, C., Galgani, F., Schmidt, N., Fauvelle, V., Brach-Papa, C., Sempéré, R., 2022. Identification and quantification of microplastics in the marine environment using the laser direct infrared (LDIR) technique. Environ. Sci. Technol. 56 (14), 9999–10009. https://doi.org/10.1021/acs.est.1c08870.

Pairaud, I.L., Gatti, J., Bensoussan, N., Verney, R., Garreau, P., 2011. Hydrology and circulation in a coastal area off Marseille: validation of a nested 3D model with observations. J. Mar. Syst. 88 (1), 20–33. https://doi.org/10.1016/j.jmarsys.2011.02.010.

Petrenko, A., Dufau, C., Estournel, C., 2008. Barotropic eastward currents in the western Gulf of Lion, north-western Mediterranean Sea, during stratified conditions. J. Mar. Syst. 74 (1), 406–428. https://doi.org/10.1016/j.jmarsys.2008.03.004.

Plastics—The Facts 2022. (s. d.). Plastics Europe FR. Accessed the 21st of September 2023, ⟨https://plasticseurope.org/knowledge-hub/plastics-the-facts-2022/⟩.

Ross, O.N., Fraysse, M., Pinazo, C., Pairaud, I., 2016. Impact of an intrusion by the Northern current on the biogeochemistry in the eastern Gulf of Lion, NW Mediterranean. Estuar. Coast. Shelf Sci. 170, 1–9. https://doi.org/10.1016/j.ecss.2015.12.022.

Ryan, P.G., Suaria, G., Perold, V., Pierucci, A., Bornman, T.G., Aliani, S., 2020. Sampling microfibres at the sea surface: the effects of mesh size, sample volume and water depth. Environ. Pollut. 258, 113413 https://doi.org/10.1016/j.envpol.2019.113413.

Santini, S., De Beni, E., Martellini, T., Sarti, C., Randazzo, D., Ciraolo, R., Scopetani, C., Cincinelli, A., 2022. Occurrence of natural and synthetic micro-fibers in the Mediterranean Sea: a review. Article 7 Toxics 10 (7). https://doi.org/10.3390/toxics10070391.

Schmidt, N., Castro-Jiménez, J., Oursel, B., Sempéré, R., 2021. Phthalates and organophosphate esters in surface water, sediments and zooplankton of the NW Mediterranean Sea: exploring links with microplastic abundance and accumulation in the marine food web. Environ. Pollut. 272, 115970 https://doi.org/10.1016/j.envpol.2020.115970.

Schmidt, N., Thibault, D., Galgani, F., Paluselli, A., Sempéré, R., 2018. Occurrence of microplastics in surface waters of the Gulf of Lion (NW Mediterranean Sea). Prog. Oceanogr. 163, 214–220. https://doi.org/10.1016/j.pocean.2017.11.010.

Schmidt, N., Castro-Jiménez, J., Fauvelle, V., Ourgaud, M., Sempéré, R., 2020. Occurrence of organic plastic additives in surface waters of the Rhône River (France). Environ. Pollut. 257, 113637 https://doi.org/10.1016/j.envpol.2019.113637.

Schmidt, N., Fauvelle, V., Castro-Jiménez, J., Lajaunie-Salla, K., Pinazo, C., Yohia, C., Sempéré, R., 2019. Occurrence of perfluoroalkyl substances in the Bay of Marseille (NW Mediterranean Sea) and the Rhône River. Mar. Pollut. Bull. 149, 110491 https://doi.org/10.1016/j.marpolbul.2019.110491.

Seuront, L., Zardi, G.I., Uguen, M., Bouchet, V.M.P., Delaeter, C., Henry, S., Spilmont, N., Nicastro, K.R., 2022. A whale of a plastic tale: a plea for interdisciplinary studies to tackle micro- and nanoplastic pollution in the marine realm. Sci. Total Environ. 846, 157187 https://doi.org/10.1016/j.scitotenv.2022.157187.

Simon-Sánchez, L., Grelaud, M., Franci, M., Ziveri, P., 2022a. Are research methods shaping our understanding of microplastic pollution? A literature review on the seawater and sediment bodies of the Mediterranean Sea. Environ. Pollut. 292, 118275 https://doi.org/10.1016/j.envpol.2021.118275.

Simon-Sánchez, L., Grelaud, M., Lorenz, C., Garcia-Orellana, J., Vianello, A., Liu, F., Vollertsen, J., Ziveri, P., 2022b. Can a sediment core reveal the plastic age? Microplastic preservation in a coastal sedimentary record. Environ. Sci. Technol. 56, 16780–16788. https://doi.org/10.1021/acs.est.2c04264.

Strady, E., Dang, T.H., Dao, T.D., Dinh, H.N., Do, T.T.D., Duong, T.N., Duong, T.T., Hoang, D.A., Kieu-Le, T.C., Le, T.P.Q., Mai, H., Trinh, D.M., Nguyen, Q.H., Tran-Nguyen, Q.A., Tran, Q.V., Truong, T.N.S., Chu, V.H., Vo, V.C., 2021. Baseline assessment of microplastic concentrations in marine and freshwater environments of a developing Southeast Asian country, Viet Nam. Mar. Pollut. Bull. 162, 111870 https://doi.org/10.1016/j.marpolbul.2020.111870.

Suaria, G., Avio, C.G., Mineo, A., Lattin, G.L., Magaldi, M.G., Belmonte, G., Moore, C.J., Regoli, F., Aliani, S., 2016. The Mediterranean plastic soup: synthetic polymers in Mediterranean surface waters. Article 1 Sci. Rep. 6 (1). https://doi.org/10.1038/srep37551.

Tesán Onrubia, J.A., Djaoudi, K., Borgogno, F., Canuto, S., Angeletti, B., Besio, G., Capello, M., Cutroneo, L., Stocchino, A., Mounier, S., Lenoble, V., 2021. Quantification of microplastics in North-Western Mediterranean harbors: seasonality and biofilm-related metallic contaminants. Article 3. J. Mar. Sci. Eng. 9 (3) https://doi.org/10.3390/jmse9030337.

Teuten, E.L., Saquing, J.M., Knappe, D.R.U., Barlaz, M.A., Jonsson, S., Björn, A., Rowland, S.J., Thompson, R.C., Galloway, T.S., Yamashita, R., Ochi, D., Watanuki, Y., Moore, C., Viet, P.H., Tana, T.S., Prudente, M., Boonyatumanond, R., Zakaria, M.P., Akkhavong, K., Takada, H., 2009. Transport and release of chemicals from plastics to the environment and to wildlife. Philos. Trans. R. Soc. B Biol. Sci. 364 (1526), 2027–2045. https://doi.org/10.1098/rstb.2008.0284.

Thompson, R.C., 2004. Lost at sea: Where is all the plastic? -838 Science 304 (5672), 838. https://doi.org/10.1126/science.1094559.

Tramoy, R., Blin, E., Poitou, I., Noûs, C., Tassin, B., Gasperi, J., 2022. Riverine litter in a small urban river in Marseille, France: plastic load and management challenges. Waste Manag. 140, 154–163. https://doi.org/10.1016/j.wasman.2022.01.015.

Tsiaras, K., Costa, E., Morgana, S., Gambardella, C., Piazza, V., Faimali, M., Minetti, R., Zeri, C., Thyssen, M., Ben Ismail, S., Hatzonikolakis, Y., Kalaroni, S., Garaventa, F., 2022. Microplastics in the Mediterranean: variability from observations and model analysis. Front. Mar. Sci. 9. ⟨https://www.frontiersin.org/articles/10.3389/fmars.2022.784937⟩.

Vousdoukas, M.I., Verney, R., Dufois, F., Pinazo, C., Sauzade, D., Meule, S., Cann, P., A. Plomaritis, T., 2011. Sediment dynamics in the Bay of Marseille, Gulf of Lions (France): hydrodynamic forcing vs. bed erodibility. J. Coast. Res. 27 (5), 942–958. https://doi.org/10.2112/JCOASTRES-D-10-00122.1.

Yohia, C., 2017. Genèse du mistral par interaction barocline et advection du tourbillon potentiel. Climatologie 13, 24–37. https://doi.org/10.4267/climatologie.1182.

Zayen, A., Sayadi, S., Chevalier, C., Boukthir, M., Ben Ismail, S., Tedetti, M., 2020. Microplastics in surface waters of the Gulf of Gabes, southern Mediterranean Sea: distribution, composition and influence of hydrodynamics. Estuar. Coast. Shelf Sci. 242, 106832 https://doi.org/10.1016/j.ecss.2020.106832.

Ziveri, P., Grelaud, M., Pato, J. 2023, Study on Actions of cities and regions in Mediterranean Sea area to fight sea pollution; Reducing marine litter and plastic pollution, REGI Committee, European Parliament, Policy Department for Structural and Cohesion Policies, Brussels.